

A novel technique for preparation of grain oriented BLSF piezoelectric ceramics

Yongxiang Li · Jiangtao Zeng · Xuezhen Jing · Qingrui Yin

Received: 11 July 2006 / Accepted: 2 April 2007 / Published online: 4 May 2007
© Springer Science + Business Media, LLC 2007

Abstract Grain oriented bismuth layer-structured ferroelectrics (BLSFs) ceramics $\text{CaBi}_4\text{Ti}_{3.95}\text{V}_{0.05}\text{O}_{15}$ were prepared by screen-printing method. The particle size of starting materials is a very important factor for the grain orientation annealed ceramics. Highly textured ceramics can only be obtained by using nanosized TiO_2 and the mechanism for grain orientation was proposed. The electrical properties of the textured ceramics showed strongly anisotropic. The dielectric constant and loss tangent in the perpendicular plane is larger than that of the parallel plane. The remanent polarization in the perpendicular plane ($2.64 \mu\text{C}/\text{cm}^2$) is also much larger than that of the parallel plane ($0.31 \mu\text{C}/\text{cm}^2$). Compared with other grain orientation techniques, screen-printing was a simple and effective technique to fabricate grain oriented BLSFs ceramics.

Keywords Bismuth layer-structured ferroelectric · Screen-printing · Grain orientation · $\text{CaBi}_4\text{Ti}_{3.95}\text{V}_{0.05}\text{O}_{15}$ · Lead-free piezoceramic

1 Introduction

Bismuth layer-structured ferroelectrics (BLSFs) are featured by their high Curie temperature and low dielectric loss [1]. It is very useful for high temperature piezoelectric applications such as high temperature accelerator. The piezoelectric properties of BLSFs are very low and many efforts have been made to improve their piezoelectricity including doping [2, 3] and the grain orientation techniques [4, 5].

Grain orientation is an effective approaching to enhance the piezoelectric properties of BLSFs. Conventionally used grain orientation techniques include hot forge (HF) [6, 7] and templated grain growth (TGG) [8, 9]. High pressure and anisotropic templates are needed for HF and TGG processes, respectively, which makes the fabrication process quite complicated.

Since the crystal grains of BLSFs are highly anisotropic [10, 11], it is possible to develop a new process to fabricate grain oriented BLSFs ceramics without using templates. We previously reported a multi-layer grain growth (MLGG) method to fabricate grain oriented BLSFs [12], but the density of ceramics were too low by using the technique. In the present work, a new process was developed to fabricate textured BLSFs with higher density.

2 Experimental procedure

$\text{CaBi}_4\text{Ti}_{3.95}\text{V}_{0.05}\text{O}_{15}$ (CBTV_{0.05}) ceramics were prepared by screen-printing method. The starting materials were analytical grade oxide and carbonate powders: Bi_2O_3 , TiO_2 , and CaCO_3 . Two types of TiO_2 powders were used in the experiment: nanosized TiO_2 and micrometer sized TiO_2 . Stoichiometric amounts of the starting powders were thoroughly mixed with ethanol in a ball mill for 4 h, then dried and calcined at 850 °C for 3 h in an alumina crucible. After calcination, the ground and ball-milled powders mixed with ethyl-cellulose and α -terpineol organic vehicle for 3 h to obtain a screen-printing paste. The paste was composed with 38 wt.% of the calcined powders and 62 wt.% of the organic vehicle. The paste was screen-printed onto a glass substrate and then dried at 90 °C, and then repeat the process 20 times until the multi-layered thick films reach about 100 μm . The films was removed carefully

Y. Li (✉) · J. Zeng · X. Jing · Q. Yin
The State Key Laboratory of High Performance Ceramics and Superfine Microstructure, Shanghai Institute of Ceramics, Chinese Academy of Sciences, Shanghai 200050, People's Republic of China
e-mail: yxli@mail.sic.ac.cn

from glass substrate and cut into $12 \times 12 \text{ mm}^2$, then, stacked in more than 20 layers, and pressed uniaxially at 100 MPa. The binder was burnt out by heating in air at a ramp of $1 \text{ }^\circ\text{C}/\text{min}$ to $600 \text{ }^\circ\text{C}$. The laminates were cold isostatic pressed at 400 MPa and then sintered at temperatures of $1,000\text{--}1,180 \text{ }^\circ\text{C}$ in air. The $\text{CBTV}_{0.05}$ powders prepared by solid-state reaction method using the same starting materials were prepared for comparison. The thickness of sample after sintering was about 1.6 mm. The samples were polished to the dimension of $10 \times 10 \times 1 \text{ mm}^3$ for electronic property measurements. Silver paste was painted on the two parallel surfaces of the tablets, and fired at $720 \text{ }^\circ\text{C}$ for 1 h.

The crystalline phase and the degree of orientation were determined by X-ray diffraction (XRD) analysis (D/max 2550V) using $\text{Cu-K}\alpha$ radiation with a scan speed of $2^\circ/\text{min}$ and a step width of 0.02° . The microstructure of the samples was observed using scanning electron microscopy (SEM, Model JSM-6700F) on the fracture surface of the samples. The ferroelectric hysteresis loops were measured by a TF Analyzer 2000 FE-Module ferroelectric tester at a frequency of 1 Hz. Dielectric constants as a function of temperature were measured with an HP4284A LCR meter at 100 kHz under a voltage of 1 V.

3 Results and discussion

3.1 XRD characterization of grain orientation ceramics

Figure 1 shows the XRD patterns of the ceramics from the screen-printing process: the plane perpendicular and parallel to screen-printing plane and the comparison with the XRD pattern of $\text{CBTV}_{0.05}$ powders by solid-state reaction. It can be seen that three XRD patterns are different. The

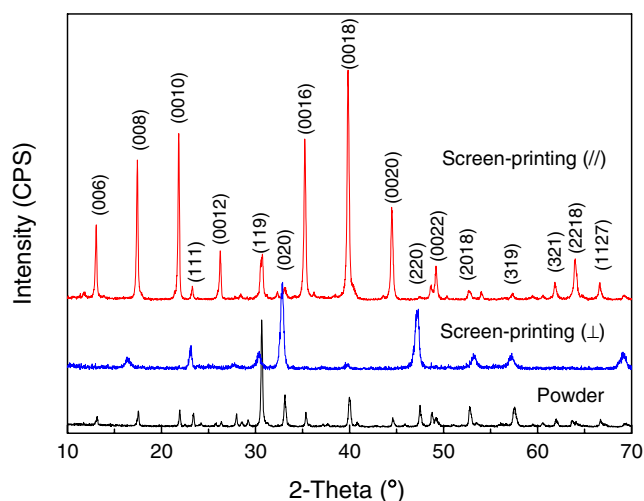


Fig. 1 The XRD pattern of the $\text{CBTV}_{0.05}$ ceramics prepared by screen-printing method on the surfaces parallel (//) and perpendicular (\perp) to the original sheet plane, compared to the XRD pattern of the $\text{CBTV}_{0.05}$ powder by conventional processing

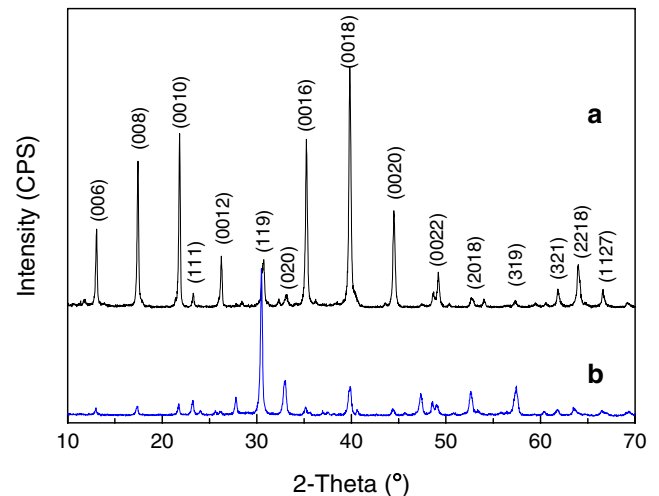


Fig. 2 XRD patterns of screen-printed ceramics with different TiO_2 : (a) nanosized TiO_2 , (b) micrometer sized TiO_2

(119) peak is the most intense peak of $\text{CBTV}_{0.05}$ powder, but it decreased remarkably and all (00l) reflections increased in the parallel plane. The (00l) reflections can hardly be observed in the perpendicular plane and (020) reflection became the most intense peak instead. This indicates that the ceramic grains were oriented align *c*-axis that is perpendicular to the screen-printing plane.

The degree of grain orientation can be calculated by Lotgering factor *f* which defined as: $f = (p - p_0) / (1 - p_0)$, where $p = \sum I(00l) / \sum I(hkl)$, $p_0 = p$ for randomly oriented sample, *f* varies from 0 to 1. The reflection lines between $2\theta = 10^\circ$ and $2\theta = 50^\circ$ were used to calculate *p* and p_0 . As a result, *f* is as high as 96% for $\text{CBTV}_{0.05}$ ceramics prepared by the screen-printing method, which is comparable to the samples prepared by hot forge and templated grain growth methods.

3.2 Particle size effect on the grain orientation

The size of starting material has great influence on grain orientation. Figure 2 shows the XRD patterns of $\text{CBTV}_{0.05}$ ceramics prepared by different size of TiO_2 particles. Using nanosized raw materials, highly oriented CBT ceramics were obtained, but when using micrometer sized TiO_2 only randomly oriented ceramics were obtained. The results indicate that grain oriented ceramics can only be obtained by using nanosized TiO_2 .

In order to illustrate the size effect more clearly, thick films prepared by nanosized TiO_2 and micrometer sized TiO_2 were laminated together and sintering at various temperatures. Figures 3(a–c) show the SEM images of ceramics prepared by such processes. The thickness of nanosized layer is about $15 \mu\text{m}$ and that of micrometer sized layer is larger than $26 \mu\text{m}$. Both layers are randomly oriented when sintered at $850 \text{ }^\circ\text{C}$, but the fracture surface of

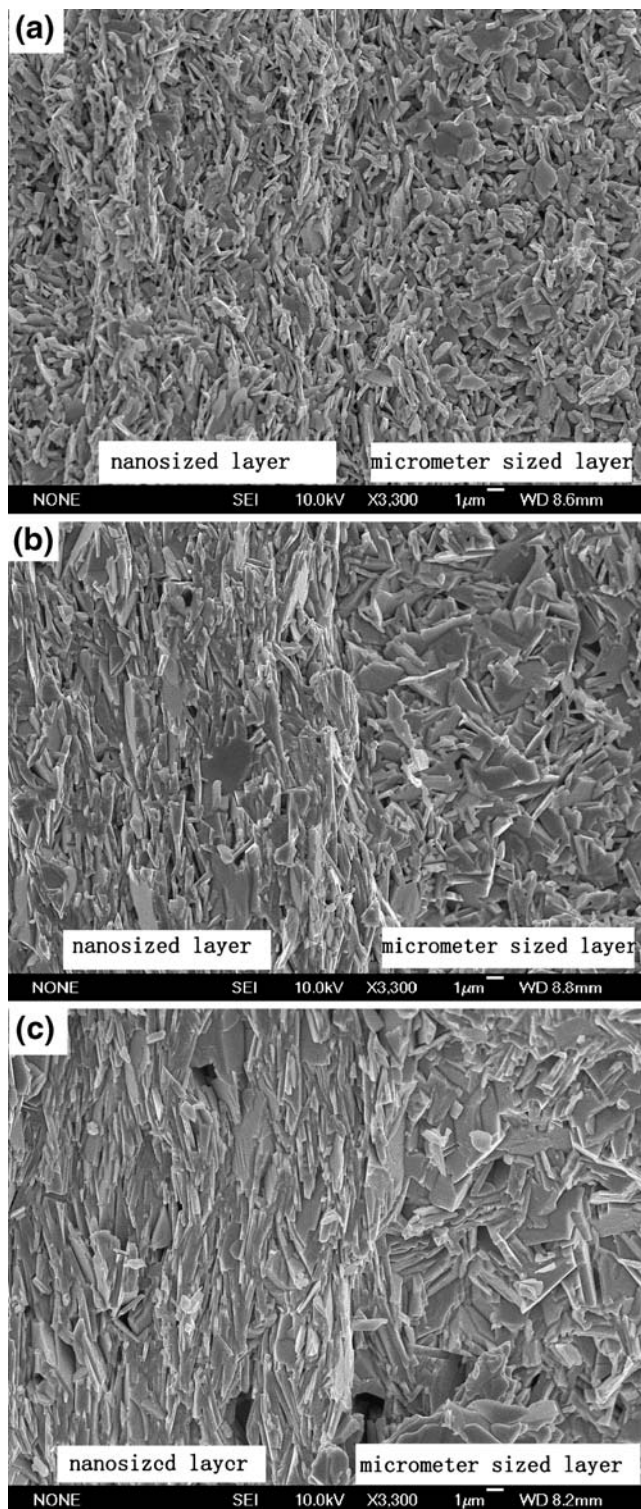


Fig. 3 SEM images of laminate with different TiO_2 sintering at (a) 850 °C, (b) 900 °C, (c) 1,050 °C

nanosized layer is quite rough compared to that of micrometer-sized layer. With the increase of sintering temperature to 900 °C, a textured microstructure developed in nanosized layer, and there are small fraction of grains randomly oriented since a few $a(b)$ planes can be seen in

this layer (as shown by arrows). In micrometer-sized layer only randomly oriented grains can be seen. When increase the sintering temperature to 1,050 °C, the grains grow large and coarse in both layers. The grain orientation degree in nanosized layer was higher than that at 900 °C.

3.3 Mechanism for grain orientation

Figure 4 shows the SEM images of dewaxed green pellet prepared by screen-printing using different TiO_2 powders. It can be seen that the shape of grains is plate-like indicating layer-structured material was synthesized after calcination. Most of the grains are randomly oriented in Fig. 4(a), but there are still some large particles which align along the screen-printing direction. Because the thickness of screen-printed film is very small, the large plate-like particles can be aligned along the screen-printing direction by the shear stress during the layer process. These particles

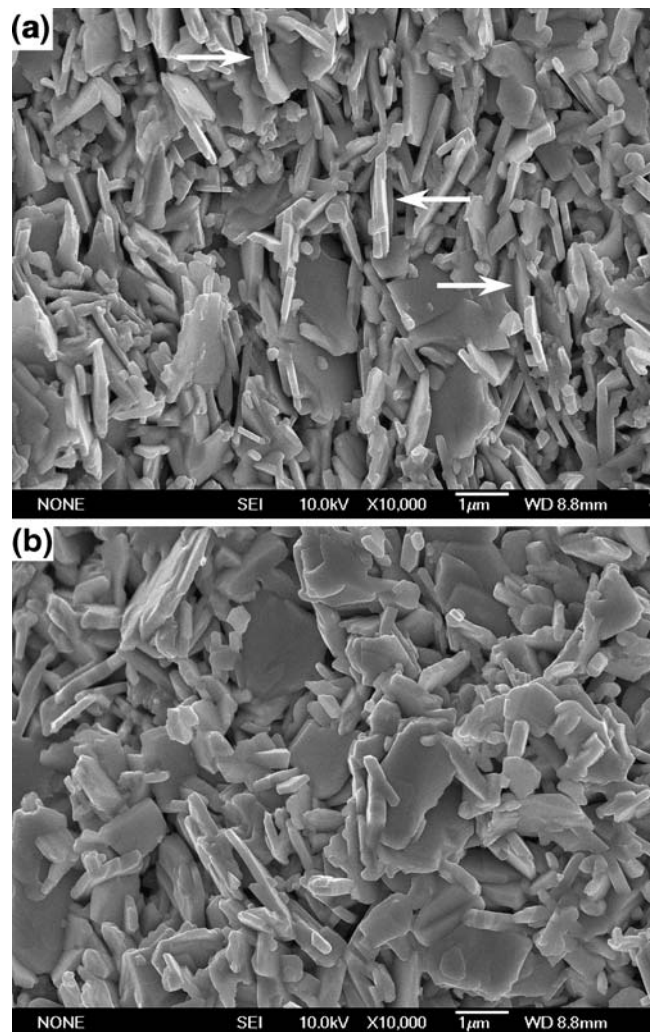


Fig. 4 SEM image of dewaxed green pellet prepared by screen-printing using different TiO_2 : (a) nanosized TiO_2 , (b) micrometer sized TiO_2

act as templates during sintering process. This process was similar to templated grain growth, but the template was synthesized in calcinations process, no need to prepare the template in advance by such as molten-salt or hydrothermal process. This is a much more simple and low cost technique compare to TGG and RTGG. In the sample prepared by micrometer-sized TiO_2 , because the screen-printed film is much thicker than that prepared by nanosized TiO_2 , plate-like particles can not be aligned along the screen-printing direction by the shear stress, consequently, only randomly grain oriented ceramics were obtained.

3.4 Dielectric and ferroelectric properties of textured ceramics

Figure 5 shows the temperature dependence of dielectric constant of prepared ceramics at two directions and randomly oriented ceramics. The inset is the enlarging of dielectric constant between R.T. and 350 °C. It can be seen that the Curie temperature was not changed by grain orientation. The dielectric constant in the perpendicular plane is higher than that in the parallel plane, and the dielectric constant of randomly oriented ceramics lies between these two planes. The difference of dielectric constant between two planes increases with the increase of temperature and reaches a maximum at the Curie temperature. The dielectric constant in the perpendicular plane is about 12 times than that in the parallel plane of c -axis. The value is very close to some single crystal BLSFs. Irie et al studied the dielectric properties of $\text{SrBi}_4\text{Ti}_4\text{O}_{15}$ and found that the dielectric constant along $a(b)$ direction is about ten times higher than that of c -axis at T_c [13].

Figure 6 shows the temperature dependence of dielectric loss of prepare ceramics in two planes and randomly oriented ceramics. The dielectric loss in the perpendicular plane is higher than that in the parallel plane. The higher

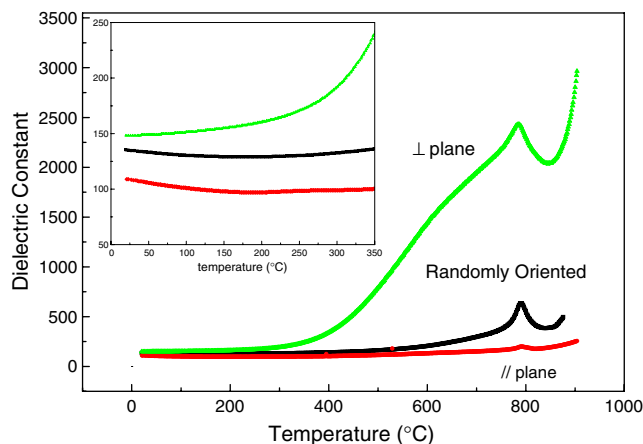


Fig. 5 Temperature dependence of dielectric constant of screen-printed $\text{CBTV}_{0.05}$ ceramics in two planes and the comparison with randomly oriented ceramics

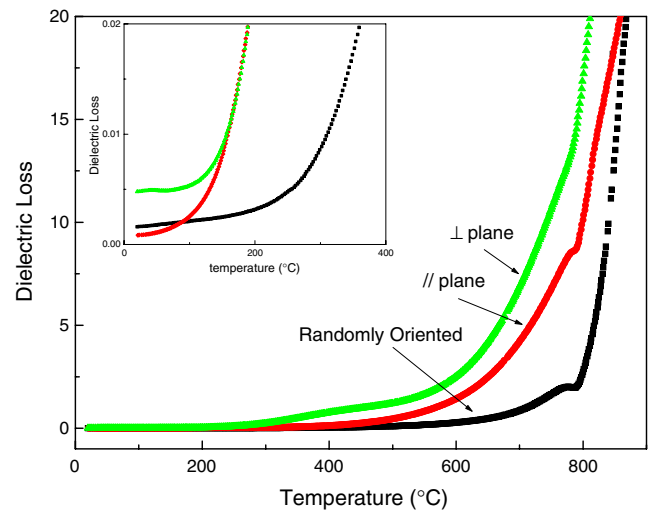


Fig. 6 Temperature dependence of dielectric loss of screen-printed $\text{CBTV}_{0.05}$ ceramics in two planes and the comparison with randomly oriented ceramics

dielectric loss in the perpendicular plane is caused by the high conductivity along $a(b)$ direction. The dielectric loss of randomly oriented ceramics lies between these two planes at low temperature, but it is lower than those prepared by screen-printing method at high temperature. The reason for the low dielectric loss of the ceramics prepared by conventional method is that they usually have higher density than that prepared by screen-printing method.

Figure 7 shows a typical P–E hysteresis curve of $\text{CBTV}_{0.05}$ ceramics at 150 °C. It is difficult to get a saturated hysteresis loop because the leakage in the perpendicular direction is quite high, but the difference of the hysteresis in two planes are obvious. The remanent polarization in the parallel plane is as low as $0.31 \mu\text{C}/\text{cm}^2$, but it is much higher in the perpendicular plane ($2.64 \mu\text{C}/\text{cm}^2$). For even number layers of BLSFs, the spontaneous polarization lies

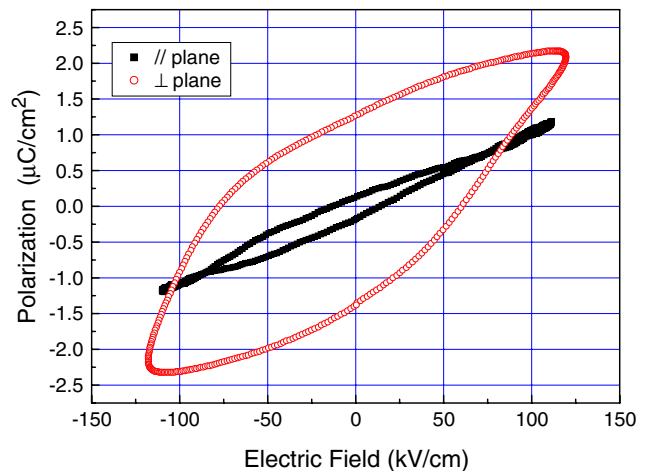


Fig. 7 P–E hysteresis loops of screen-printed $\text{CBTV}_{0.05}$ ceramics in two planes

along $a(b)$ direction, and no polarization along the c -axis due to a mirror symmetry. CBTV_{0.05} ceramics prepared by screen-printing have the c -axis perpendicular to the screen-printing plane, so the perpendicular plane was expected to have better piezoelectric properties.

4 Conclusion

Screen-printing method was used to prepare textured BLSFs CaBi₄Ti_{3.95}V_{0.05}O₁₅ ceramics. The XRD and SEM results showed strong preferred grain orientation. The particle size of starting materials plays a crucial role for the grain orientation. Highly textured ceramics can only be obtained by using nanosized TiO₂ and the mechanism for grain orientation was similar to TGG method, but the template was formed during calcinating process. The electrical properties of so made textured ceramics showed strong anisotropic. The dielectric constant and loss in the perpendicular plane is larger than that in the parallel plane. The remanent polarization in the perpendicular plane is also much larger than that in the parallel plane. Without the use of template particles and pressure densification process, the screen-printing is a simple approach to fabricate grain-orientated piezoceramics.

Acknowledgements This work was supported by the Ministry of Sciences and Technology of China through 973-project (2002CB613307), National Natural Science Foundation China (NSFC No. 50572113), and the Innovation Project of Shanghai Institute of Ceramics (SCX200409).

References

1. E.C. Subbarao, J. Phys. Chem. Solids. **23**, 665–676 (1962)
2. M. Villegas, T. Jardiel, G. Farias, J. Eur. Ceram. Soc. **24**, 1025–1029 (2004)
3. H. Maiwa, N. Iizawa, D. Togawa, T. Hayashi, Appl. Phys. Lett. **82**, 1760–1762 (2003)
4. M. Holmes, R.E. Newnham, L.E. Cross, Am. Ceram. Soc. Bull. **58**, 872 (1979)
5. T. Takenaka, K. Sakata, J. Appl. Phys. **55**, 1092–1099 (1984)
6. T. Takenaka, K. Sakata, Jpn. J. Appl. Phys. **19**, 31–39 (1980)
7. T. Kimura, T. Yoshimoto, N. Lida, J. Am. Ceram. Soc. **72**, 85–89 (1989)
8. T. Takeuchi, T. Tani, Y. Saito, Jpn. J. Appl. Phys. **38**, 5553–5556 (1999)
9. J.A. Horn, S.C. Zhang, U. Selvaraj, J. Am. Ceram. Soc. **82**, 921–926 (1999)
10. H. Amorin, V.V. Shvartsman, A.L. Kholkin, M.E. V. Costa, Appl. Phys. Lett. **85**, 5667–5669 (2004)
11. S. Kim, M. Miyayama, H. Yanagida, J. Ceram. Soc. Jpn. **102**, 722–726 (1994)
12. J.T. Zeng, Y.X. Li, Q.B. Yang, J. Eur. Ceram. Soc. **25**, 2727–2730 (2005)
13. H. Irie, M. Miyayama, Appl. Phys. Lett. **79**, 251–253 (2001)